Preliminary Laboratory Performance of the NCT Prototype Flight Electronics

Wayne Coburn[a], Steven E. Boggs[a,b], Julia M. Kregenow[a], Jason D. Bowen[a],
Mark S. Amman[c], Morgan T. Burks[e], William Craig[e], Pierre Jean[d], Robert P. Lin[a,b], Paul N.
Luke[c], Norman W. Madden[e], David M. Smith[a], Peter von Ballmoos[d], Klaus Ziock[e]

[a]Space Sciences Laboratory, University of California, Berkeley, CA 94720, USA
[b]Department of Physics, University of California, Berkeley, CA 94720, USA
[c]Lawrence Berkeley National Laboratory, University of California, Berkeley, CA 94720, USA
[d]Centre d'Etude Spatiale des Rayonnements, CNRS/UPS, BP 4346, 31029 Toulouse Cedex,
France
[e]Lawrence Livermore National Laboratory, Livermore, CA 94550, USA

ABSTRACT

We are developing a 2-detector high resolution Compton telescope utilizing 3D imaging germanium detectors (GeDs) to be flown as a balloon payload in Spring 2004. This instrument is a prototype for the larger Nuclear Compton Telescope (NCT), which utilizes 12-GeDs. NCT is a balloon-borne soft γ–ray (0.2–15 MeV) telescope designed to study, through spectroscopy, imaging, and timing, astrophysical sources of nuclear line emission and γ–ray polarization. The NCT program is designed to develop and test the technologies and analysis techniques crucial for the Advanced Compton Telescope, while studying γ–ray radiation with very high spectral resolution, moderate angular resolution, and high sensitivity. NCT has a novel, ultra-compact design optimized for studying nuclear line emission in the critical 0.5–2 MeV range, and polarization in the 0.2–0.5 MeV range. The prototype flight will critically test the novel instrument technologies, analysis techniques, and background rejection procedures we have developed for high resolution Compton telescopes. In this paper we present the design and preliminary results of laboratory performance tests of the NCT flight electronics.

Keywords: Germanium detectors; gamma-ray spectroscopy; gamma-ray astronomy; gamma-ray polarization; balloon payloads

1. INTRODUCTION

The *Nuclear Compton Telescope* (NCT) is a balloon-borne soft γ–ray (0.2–15 MeV) telescope designed to study astrophysical sources of nuclear line emission and γ–ray polarization (1; 2). It employs a novel Compton telescope design (Fig. 1), utilizing *twelve* high spectral
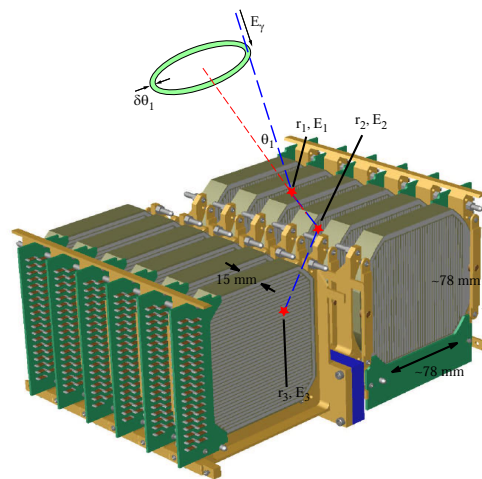
Further author information:
E-mail: wcoburn@ssl.berkeley.edu,
Telephone: 1 510 643 1855

Figure 1. The heart of NCT is an array of 12 cross-strip GeDs with 3-D position resolution, excellent spectroscopy, sensitivity to γ–ray polarization, and high efficiency.

resolution germanium detectors (GeDs) with the ability to track the location in three dimensions of each photon interaction. The tracking serves three purposes: imaging the sky using Compton imaging techniques, measuring polarization, and very effectively reducing background.

The entire set of detectors and their cryostat is enclosed inside an active BGO well, giving an overall field of view of 3.2 str. The instrument is mounted in a pointed, autonomous balloon platform and is capable of long duration ($\sim$2 week) balloon flights. NCT is designed to optimize sensitivity to nuclear line emission over the crucial 0.5–2 MeV range, and sensitivity to polarization in the 0.2–0.5 MeV range. The guiding principle of NCT is that high efficiency and excellent background reduction are critical for advances in soft γ–ray sensitivity.
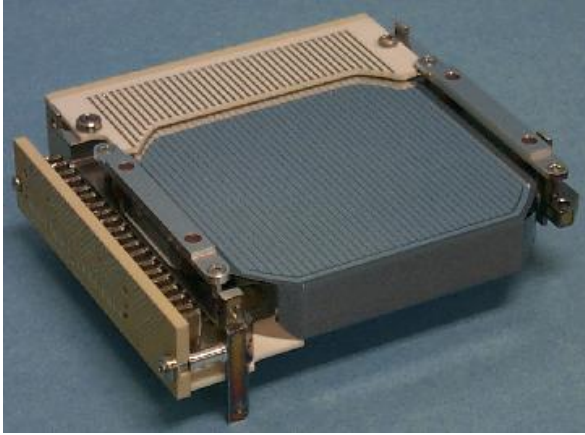
Figure 2. Photograph of one of our two flight detectors. Each detector has 37×37 strips, and an active volume of $82.1\,cm^3$ containing over 41-thousand pixel-volume elements used to track each incident γ-ray as it scatters through the detector.

Figure 3. NCT flight preamps in their shielded housing, with 10 compact preamps per board, four boards per GeD face. (The top cover has been removed and flipped to show how each preamp is electrically shielded for low noise.)

The sensitivity of NCT is signal-limited, *not* background limited. This means that NCT will explore a new phase space of source-dominated nuclear γ-ray observations. Some of the long term goals of NCT include mapping both ^{26}Al and ^{60}Fe in the plane and bulge of our galaxy, measuring the amount of ^{44}Ti contained in recent core collapse supernova remnants, measuring with high resolution the spectra of AGN and searching for γ-ray polarization, looking for polarization in the emission from pulsars and associated plerions, and searching for redshifted deuterium lines from the surfaces of neutron stars.

At the heart of the NCT in an array of large volume, 3-D positioning cross strip GeDs, which are being developed using LBNL's amorphous Ge contact technology (3). For characterizing our electronics we used a 19×19 strip GeD, 11 mm thick, p-type planar prototype detector. Orthogonal strips were deposited on both faces of the GeD, with a strip pitch of 2 mm and a 0.5 mm gap between strips. The strips define an active area of $14.4\,cm^2$. A 4 mm wide guard ring surrounds this active area on both faces of the detector. The depletion voltage is -1600 V, and we operate the GeD at -2000 V. We instrumented the strips on both the ground (DC coupled, anode side) and HV (AC coupled, cathode side) sides with custom low power, low noise preamplifiers (4). This preamp, which utilizes predominantly surface mount components, achieves excellent spectroscopic performance with a small footprint and at a modest cost.

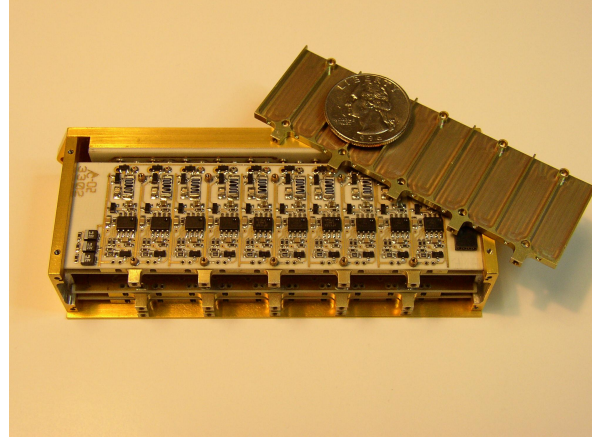For the prototype balloon flight, we will use two GeDs

that are similar to yet larger than our prototype detector (Fig. 2). Each of the flight detectors have 37×37 strips, and are 15 mm thick. The strip pitch is the same, 2 mm, but with a 0.25 mm gap to help reduce the effects of charge sharing between strips. The guard rings are 2 mm thick, with a 1 mm gap between the ring and the edge of the crystal. The preamps we are using are of the same design as those used for the prototype detector. A photograph of one of our 40 preamplifier packages is show in in Fig. 3.

In §2 we give a brief description of our flight electronics. In §3 we examine the current state of the 3D-positioning of those electronics. In §4 we discuss the spectral uniformity of our flight electronics across both strips and pixels using our prototype detector. Finally, we finish in §5 with a brief discussion of our future work and the upcoming balloon flight.

2. DETECTOR ELECTRONICS

NCT uses conventional GeD quality signal processing electronics. Each detector strip has a compact, low power signal processing chain made predominantly of conventional surface mount components. Detector signal extraction is accomplished with a unique charge sensitive preamplifier (Fig. 3), in which excellent spectroscopic performance is achieved in a small footprint and at modest cost and low power, without sacrificing signal bandwidth (5). A much-simplified pulse-shaping amplifier, with both a fast and slow channel, follows each preamplifier. The slow channel, iwth a $8\,\mu s$ peaking time, is followed by a peak detect and stretch function. The fast channel uses a small delay
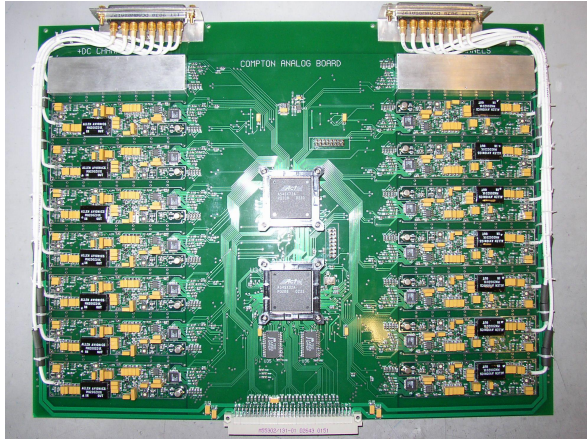
Figure 4. NCT flight signal processing board, with 16 channels per board, 5 boards per GeD, and two ACTELS, one for coincidence logic, and the second for collecting rates in each channel. (Electric shield covers are removed from all but two channels.)

line constant fraction discriminator to time stamp each waveform at 50% of its maximum amplitude, generating a low time walk signal. Demonstrated resolutions are 1.2 keV FWHM spectral resolution at 60 keV, and 0.5 mm FWHM depth determination for all interactions that deposit ≥20 keV. Spectroscopy signals uniquely match the fast-signal pairs for multiple interactions in the same GeD.

One 16-channel signal-processing cluster resides on a single printed circuit card (Fig. 4), with both the fast and slow analog signal processing electronics. Five cluster boards are required for each GeD. The cluster connects into a common back plane, which supplies bi-directional housekeeping communication, power, and event data channels. Low level input signals connect to the front panel well away from the back plane. Each card has two ACTEL Field Programmable Gate Arrays (FPGA), one which keeps track of the LLD, ULD and fast trigger rates in each strip, and the second which co-ordinates the logic between the slow and fast channels, as well as the shield veto signals. A single DSP for each detector interfaces between the 5 identical ACTEL sets for each cluster and the main flight computer. The total power per channel is 210 mW, for a total consumption of 197 W for the full 12-GeD instrument.

3. 3D POSITIONING

There are two main keys to Compton imaging with this system. The first is to accurately determine the energy deposited in the detector at each interaction. The second is successfully tracking, in all three dimensions, the
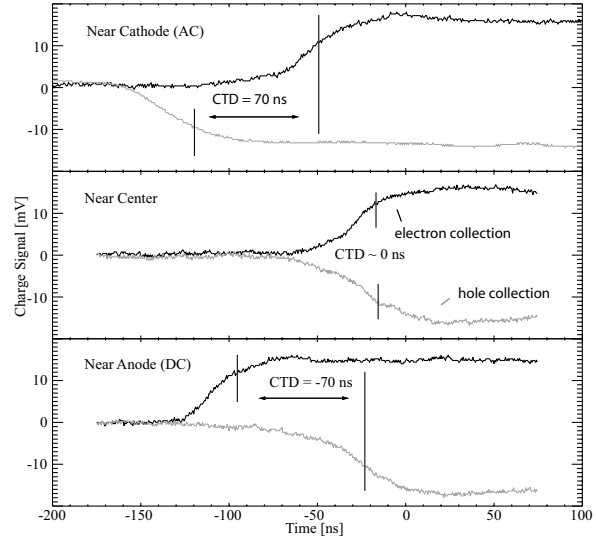

Figure 5. Induced signals on anode and cathode strips of our prototype GeD, for 122 keV photon events near the anode (top), the GeD center (middle), and the cathode (bottom). Our 3-D electronics use a simple delay line to time-tag each strip signal as it crosses 50% of its maximum amplitude.

γ−ray interactions within the detector. When a photon interacts in a GeD, either by photoabsorption or Compton Scattering, a fast recoil electron is produced which knocks more electrons from the valence band to the conduction bad, leaving holes behind. The number of e-h pairs is directly proportional do the energy deposited (1 e-h pair per 2.98 eV). In an applied electric field (bias voltage), these e-h pairs will separate and drift in opposite directions, electrons toward the anode and holes toward the cathode. By segmenting the anode into strips, and the cathode into orthogonal strips, 2-D positioning is achieved directly through identification of the active anode and cathode strips.

Measuring the "depth", or "z position", of the interaction in the detector (the distance between the γ−ray interaction and either the anode or cathode strip), is achieved by measuring the difference between electron and hole collection times on opposite faces of the detector (see Fig. 5). The Collection Time Difference (CTD) for an event is well defined, and has been shown to be linear with depth to first order (6; 7). The drift time across an 11 mm thick GeD is on the order of 100 ns.

To characterize this effect, we used bench-top electronics, a collimated source, and a fast oscilloscope to digitize the charge collection signals on two crossed strips (see Fig. 5). Our analysis of the charge collection times show that it is possible to achieve our re-
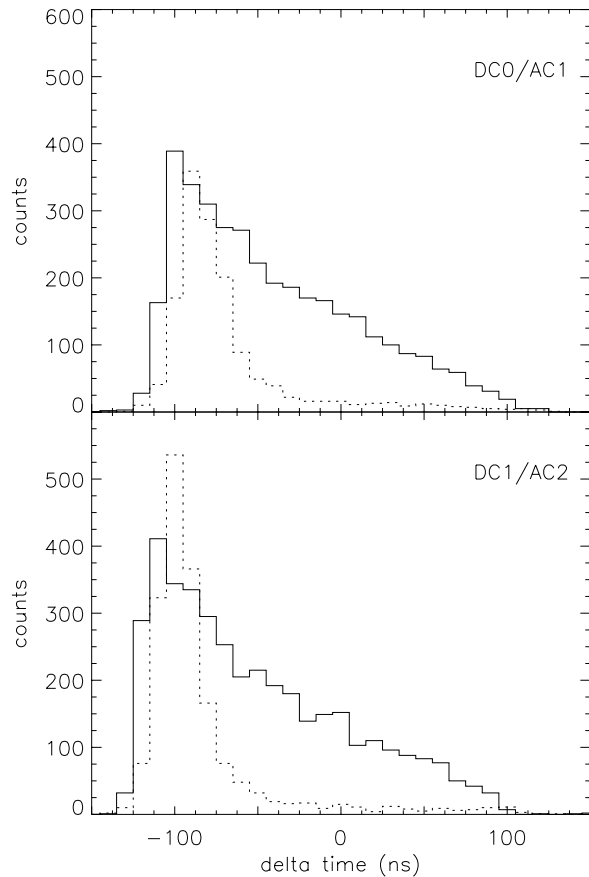
Figure 6. Distribution of charge time differences (DC channel time minus AC channel time) using the NCT flight electronics and at 122 keV (solid line) and 60 keV (dotted line). The detector was illuminated from the DC side. AC illumination of the detector produces similar plots, however the peaks occur at +100 ns instead of -100 ns. TOP: Data using DC-channel 0 and AC-channel 1. BOTTOM: DC-channel 1 and AC-channel 2. These plots are representative of what is expected for each cross strip pair and in each detector.

Figure 7. Calibrated depth distributions for both DC and AC illumination by sources at three photon energies: (TOP) 60 keV, (MIDDLE) 122 keV, and (BOTTOM) 662 keV. Simple exponential attenuation curves are shown for comparison.

quired <1 mm depth resolution for 60 keV interactions (7). This resolution improves with increasing energy, until the recoil electron stopping length becomes significant.

While this system works well, digitizing the charge signals for the NCT balloon flight instrument is impractical due to the power and size constraints. Instead, we have developed a simple analog constant fraction discriminator which records the time when each channel signal reaches 50% of its maximum amplitude (8). Our analog electronics have achieved an 0.5 mm FWHM resolution at 60 keV - which is comparable to the digitizing technique, but with a much smaller, simpler, lower power system.
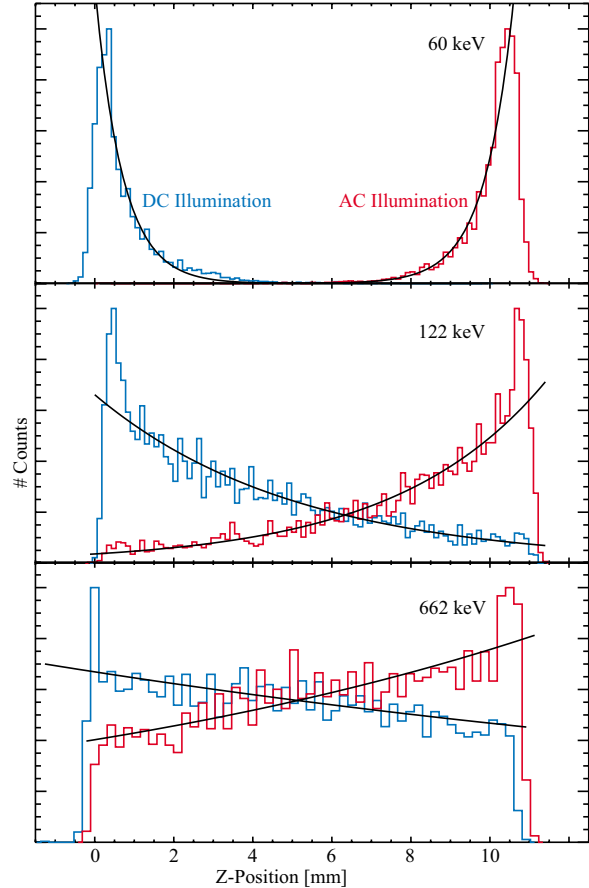
In Fig. 6 we she the results of tests using our flight electronics for two nearly representative cross strip pairs. The calibration of the interaction depth in terms of the CTD poses a unique problem since we cannot send in events of known depth. We can, however, send in events with a known depth distribution. In an ideal detector, a histogram of CTDs would have a step-function rise and peak at the charge crossing time of the detector (corresponding to photons interacting a the surface of one side), and exponentially decay away with increasing depth. This exponential decay should follow the known attenuation for a photon at that energy in germanium. Our prototype detector shows some surface effects, but these are well characterized and understood using Monte Carlo simulations (7; 9).

The conversion of CTDs to depth, or z position, is discussed in detail in (7) and (9). When we illuminate

both sides (AC and DC) of the detector with photons of the same energy, the distribution in depth on the two sides should be the same. Since the charge propagation time in the detector should not depend on the incident photon energy, we also require that the same calibration curve simultaneously result in uniformity between the sides at many different photon energies. As an independent verification of our results, the best fit mean free paths on both sides of the detector using the calibration will not only have to be identical, but also have to agree with known values for germanium. This technique has worked successfully with a test version of the flight electronics, and we will apply it to every cross strip pair once the full set of flight electronics has been fabricated.

4. SPECTRAL PERFORMANCE

Since our GeDs are cut from a single, homogeneous germanium crystal, their efficiency, spectral resolution, and position resolution are uniform across the face of the detector (9). Variations between strips are generally on the few percent level, and easily calibrated. Fig. 8 shows the results of a collimated scan of our prototype detector, demonstrating the excellent uniformity of the germanium crystal photopeak efficiency.

Maintaining this uniformity with our flight electronics, as opposed to benchtop electronics, is a high priority in our electronics development and testing. The success of our science objectives requires all 16 channels (8 anode, or DC, and 8 cathode, or AC) on each of the 5 flight boards for each detector provide similar response. With guard rings, this is a total of 152 channels for the 2-GeD prototype flight, and 912 channels for the full NCT system.

There is still some testing, calibrating, and minor design changes (mostly in the software of the readout system) that need to be done before our system is fully optimized and the remaining flight boards can be fabricated. The electronics are, however, currently working quite well. In Fig. 9 we show the results of illuminating the prototype detector with a ^{57}Co source. The 8 DC channels were connected to 8 consecutive anode detector strips, and the spectra obtained simultaneously. The data came through the through the entire flight system, with packetized data read by a GSE computer rather than the main gondola flight computer.

The total numbers of 122 keV photopeak events recorded for each channel in Fig. 9, while not statistically equivalent to a single counting rate, are quite similar to each other. The extremes range ±2.7% from
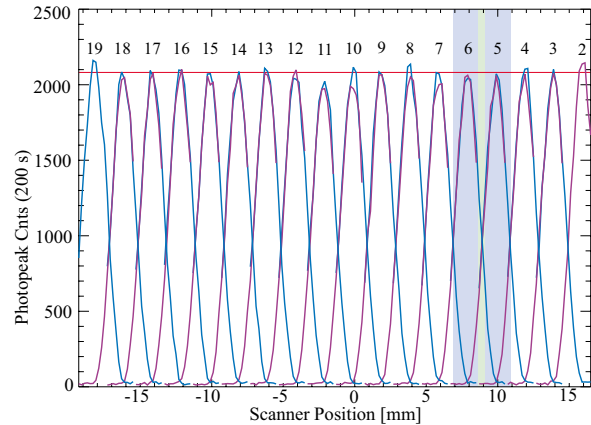

Figure 8. Scan across the DC strips in our strip prototype detector using a 0.5 mm collimated ^{241}Am (59.5 keV) source. This nicely demonstrates the uniformity of the Ge crystal. Channel 1 was improperly instrumented at the time of these scans, and therefore is missing. The average peak height is shown (horizontal line), as well as strips representing the geometrical area of the metallic contacts (dark grey) and the gap between (light grey).

the average, which makes flat field calibrations of the detector relatively simple and straight forward.

The spectral resolutions of each of the anode channels taken with the flight electronics are quite good. On average, the the resolutions obtained with the flight board are identical to what we get using benchtop electronics. The range of values obtained with the flight board (±12%) is also similar to the range seen with lab equipment (±8%). All of these tests were done before optimizing the pole zero, gain, and threshold of each electronics channel for each anode strip. Therefore we are confident we will be able to obtain spectral resolutions in our flight detectors with flight electronics that are similar to what we get in the lab.

In Fig. 10 we show the results of a similar test, only this time using a ^{241}Am source with a 59.5 keV characteristic X-ray. Again, and with the exception of channels 6 and 7 (see below), the total photopeak events are quite similar (the extremes being only ±7% of the average). When compared with benchtop electronics the average spectral resolution obtained is 6% worse. This can, however, be attributed to an apparent problem with DC channel 0 at the time of this test.

The lower counting rates in channels 6 and 7 can easily be understood in terms of the fast lower level discriminators (FLLDs) in our electronics. Just as in the ^{57}Co data run, the the settings of the electronics channels have not been optimized for each detector strip.
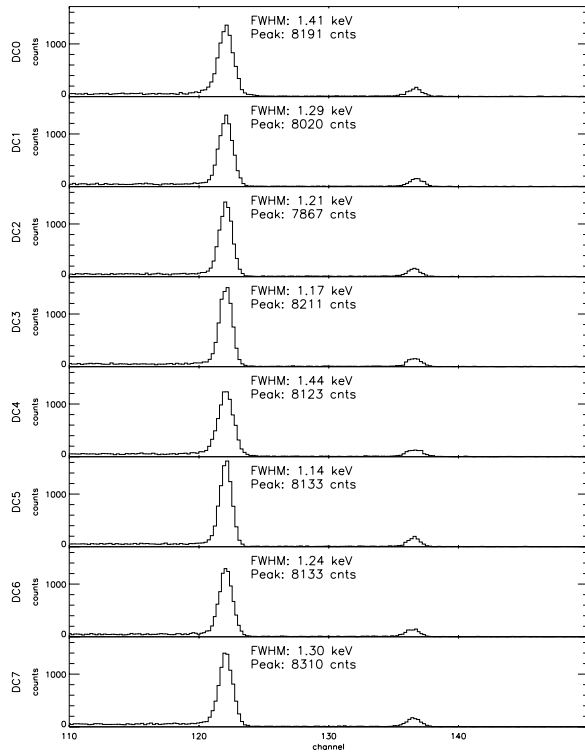
Figure 9. Anode side strip spectra of 8 individual strips using the 8 Anode channels in our flight electronics when illuminated with a ^{57}Co source. The 122 keV and 136 keV lines can be clearly seen in the eight spectra. The 122 keV FWHM and integrated photopeak counts are given in each panel, and are roughly consistent with being uniform.

Figure 10. Similar to Fig. 9, but with a ^{241}Am source. The characteristic 60 keV line can be clearly seen in each electronics channel, however it is suppressed somewhat in channels 6 and 7. This is due to the ∼60 keV thresholds in the fast channles of these two electronics chains.

In the case of channels 6 and 7, the FLLDs are currently set close to 60 keV. Since our coincidence logic currently requires FLLD triggers on both anode and cathode sides of the detector, many of the 60 keV photons that interact in the strips associated with channels 6 and 7 are below the threshold and therefore fail to generate a trigger. This is why we do not see a similar problem at 122 keV, an energy that is well above all of the FLLDs. The FLLDs on the other channels (0–5) are lower, but there are still some events that fail to provide a valid trigger. This is why there is a broader range in the numbers of photopeak counts in these channels when compared to the ^{57}Co data ($\pm 7\%$ instead of $\pm 2.7\%$). Once the electronics have been fully tested and optimized for each strip, the FLLDs should be considerably lower. The design goal was to have all of the FLLDs set to 50 keV, but given what we have seen in the lab we feel that 30 keV or less should be obtainable.
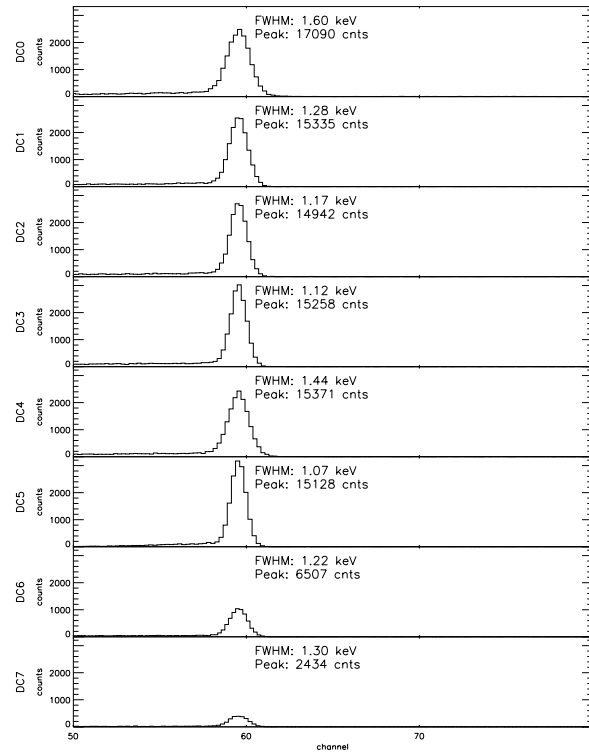
With a set of 8 anode and 8 cathode cross stip events,

spectra of a given x/y position can be generated. In Fig 11 we show an array of 64 cross strip, or pixel, spectra using the same dataset as in Fig. 9. The ^{57}Co source was ∼ 1 m from the detector, giving a nearly uniform illumination of each detector strip. Only anode events were used in binning each spectra. Cathode events, which provide redundant spectral information, were only used to identify which AC strip to associate the photon with.

With the exception of those events associated with AC channel 0, each of the pixel spectra in Fig. 11 are remarkably similar. Just as in the strip spectra, the integrated counts under each 122 keV photopeak and the spectral resolutions are similar for each pixel. Since every anode event that was above the threshold is in each spectra, the effects of charge sharing would be evident and appear as tailing below the photopeak energy. As expected (9), we do not see any significant tailing in the spectra. The lower counting rate in AC channel 0 is due to the FLLD of that channel being set near the incident photon energy.
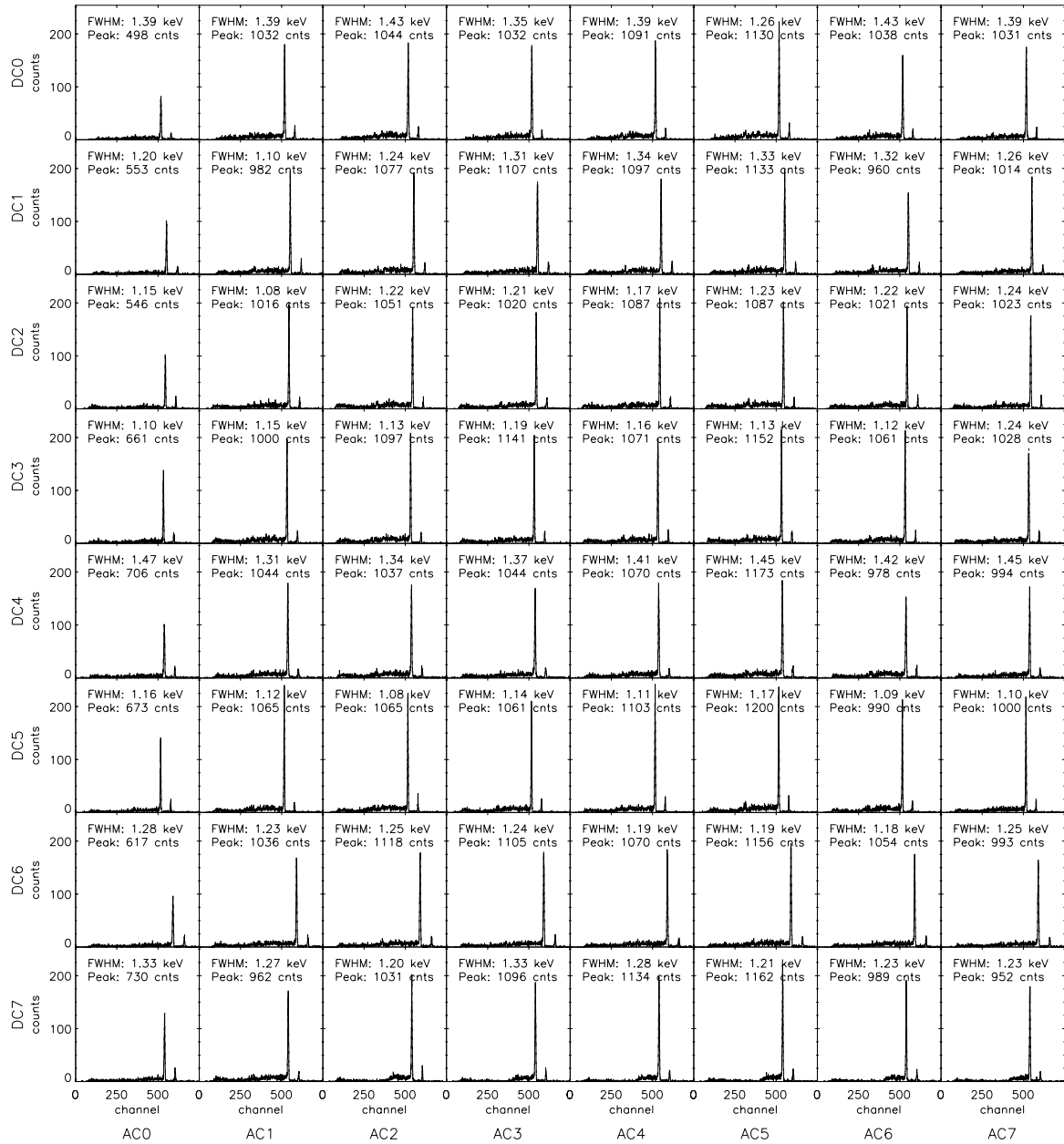
Figure 11. A complete set of anode spectra for each cross strip pair (pixel) using the current set of 8 anode (DC channel) and 8 cathode (AC channel) electronics. The pixels associated with AC channel 0 have fewer counts than expected. This is due to fewer counts being collected through AC0 itself, which was caused by the FLLD in this channel being set near the incident photon energy.

Figure 12. NCT flight cryostat during integration tests with the BGO shields into the instrument cradle. The entire cradle assembly pivots to allow pointing at different elevations.

5. FUTURE WORK

We are currently finishing the fabrication of the two 37×37 strip flight detectors. We have almost finished testing the first of the flight electronics boards, and will soon be fabricating 10 more. The DSP board, which coordinates the outputs of the 5 electronics boards and passes packetized data to the main gondola flight computer, is currently working. Once we have a full working 2-GeD system, with detectors and a full set of flight electronics, we will begin a series of tests and calibrations to fully characterize the optimize the overall detector performance.

The balloon platform itself, which borrows heavily on HIREGS LDBF heritage, is nearly ready for flight. In Fig. 12 we show a photograph of the integration of the flight cryostat into the shield assembly. The shield pieces and electronics have been tested since the last HIREGS balloon flight, and the entire system working as expected. Only minor modifications to the flight computer hardware and software need to be made to integrate it into the new detector system. The GSE hardware is in place, and the GSE software currently under development. We plan on flying this NCT prototype on a conventional continental US balloon flight from Fort Sumner, New Mexico, in the Spring of 2004.

ACKNOWLEDGMENTS

References

[1] S. E. Boggs *et al.* in *Gamma 2001, AIP Conf. Proc.*, 587, p. 877, 2001.

[2] S. E. Boggs *et al.* in *IEEE NSS Conf. Proc.*, N14-5, 2001.

[3] P. N. Luke *et al.* in *IEEE Nucl. Sci. Symp. Conf.*, 39, p. 590, 1992.

[4] L. Fabris, N. Madden, and H. Yaver *NIM* , p. A424, 1999.

[5] L. Fabris, N. Madden, and H. Yaver *NIM* A424, p. 545, 1999.

[6] M. Amman and P. N. Luke *NIM* A452, p. 155, 2000.

[7] S. Amrose *et al.* in *IEEE NSS Conf. Proc.*, N12-22, 2001.

[8] M. T. Burks *et al.* in *IEEE Nuclear Science Symposium*, November 2001.

[9] W. Coburn *et al. SPIE* 4784, p. 54, 2002.